

## SEASONAL TEMPERATURE VARIATION OF SOLAR POND UNDER MEDITERRANEAN CONDITION

by

**Haci SOGUKPINAR**

Department of Electric and Energy, Vocational School, University of Adiyaman, Adiyaman, Turkey

Original scientific paper  
<https://doi.org/10.2298/TSCI180518060S>

*In this paper, thermal performance of solar pond for different condition was numerically investigated by using discrete ordinates method to facilitate a greater understanding of the effects of relative various condition on thermal performance improvement of solar pond. For this, a 3-D prototypes of solar ponds with square cross-sections were simulated for the oversoil and subsoil, insulated and uninsulated, open on and off conditions. The direction of sunlight (zenith angle and the solar elevation) was automatically computed from the latitude, longitude, time zone, date, and time. The estimated solar position is accurate for a date between year 2000 and 2199, due to an approximation used in the Julian Day calendar calculation. Seasonal temperature variation of solar pond was calculated for the full period of one year starting from March and calculated data were compared with experiment to validate simulation accuracy of heat transfer model. Result indicates that temperatures in the summer time were calculated at around 55 °C, while temperatures in the winter were in the range of 20 to 30 °C and temperature changes between 30 °C and 40 °C in spring and autumn.*

Key word: *seasonal variation, solar pond, comsol, performance of solar pond*

### Introduction

Solar energy travels to the earth surface in the form of electromagnetic radiation is selectively absorbed, transmitted and scattered as it goes through atmospheric layers, and finally heats up everything around the surface and provide energy for all the processes of life. Today, the world's energy needs is met from different sources however, the use of clean energy resources is important to live in a cleaner environment. Because the effects of global warming have begun to be seen in everyday life and climate changes are affecting our lives negatively. Therefore, world countries, especially Europe, are investing heavily for the most efficient use of RES. Solar energy is the most potent RES from these and can be converted into different forms of energy using different technologies. Solar ponds are one of these technologies and are used to produce water at a low temperature by using cheaper technology without polluting the nature. It is possible to obtain hot water up to 60 °C in a solar pond, constructed by using salt water with different density [1] and generated heat can be used directly for a wide range of application such as generation of electricity, heating the environment, meeting the need of hot water, drying food and obtaining fresh water from salty water. Since the geographical locations of the countries, and therefore the solar view angle is different and the periods of solar shine durations vary. Countries close to the equator are advantageous while countries close to the

polar are falling to disadvantage. Due to cyclic nature and time-dependency of the solar energy, usage has not commercialized in many countries [2]. In recent 20 years, a number of theoretical and experimental studies have been carried out on the performance of solar ponds in order to understand its mechanism and to make it available to the community. Overall energy and exergy efficiencies of the salinity gradient solar pond was investigated numerically and exergetic performance analysis of a solar pond was calculated [3]. The effect of sunny area ratios on the thermal performance of solar ponds was investigated and study showed that careful determination of the boundaries, insulation parameters and rate of incoming solar radiation reaching the storage areas has increased the efficiency of the solar pond [4, 5]. A mathematical model was developed to investigate thermal performance of solar pond by introducing nanofluid solar pond [6]. For this, upper zone of the pond is made of mineral oil but the lower side is formed with excellent solar radiation absorber which is nanofluid materials. Investigation showed that because of better solar absorption properties, nanofluid materials have better solar energy storage capacity than a traditional salinity gradient solar pond. On the other hand, salinity-gradient solar pond uses a large amount of saltwater as a medium for collecting and storing solar heat from the sun and this makes the system installation cheap and easy [7]. Numerous experimental and theoretical studies were about the performance analysis of salinity gradient solar pond [8-14]. Some of these studies concentrated on functioning and mechanism of solar pond but some others only the cases insulated or uninsulated conditions, some of them related with or without cover, some others investigated above ground and subsoil conditions of solar pond. To evaluate thermal efficiency of solar pond several model were developed based on conservation principle of thermodynamic [15-18]. With the help of the different models, the temperature distribution in the solar pond, the heat losses from the side wall, floor and the surface can be calculated to be compatible with the experimental data.

In this study, numerical calculations were conducted for 3-D model solar pond to calculate thermal efficiency for the cases such as insulated and uninsulated, oversoil and subsoil, and with and without cover. For this, a prototypes of solar ponds with square cross sections were simulated and calculated data were compared with experimental data to validate simulation accuracy of heat transfer model.

### Numerical approaches

Although different liquids or heat holders are used, solar ponds are built in the most economical way by using salt water. By using layers of saline with different densities, the inter-mixing of water between the layers is energized, and heat is trapped inside. In fact, solar pond has been discovered by measuring significant differences in depth-dependent temperature gradients in salt water lakes. When the side walls and the floor are insulated, the heat stored in the bottom layer cannot mix with the top layers, so heat loss is minimized. In order to make an efficient solar pond in terms of heat storage, it must have at least three zone. As shown in fig. 1(a), each layer convects in itself, but does not interfere with other layers, in this way a natural isolation occurs. The upper zone is called the upper convective zone (UCZ) and the temperature of this zone is the same as the outside. Because this zone is in direct contact with the air and natural convection on the outside immediately absorbs the heat of this layer but the middle layer serves as an isolation between the upper and inner layers, and this zone is called the non-convective zone (NCZ). The temperature distribution of this layer varies between the UCZ and the inner zone temperature. The number of zones of the NCZ can be increased to maximize protection of heat in the inner layer. Due to this reason NCZ consists of 5 different zones for this study as shown in fig. 1(b). The bottom zone is called the heat storage zone (HSZ) where maximum amount of heat is stored.

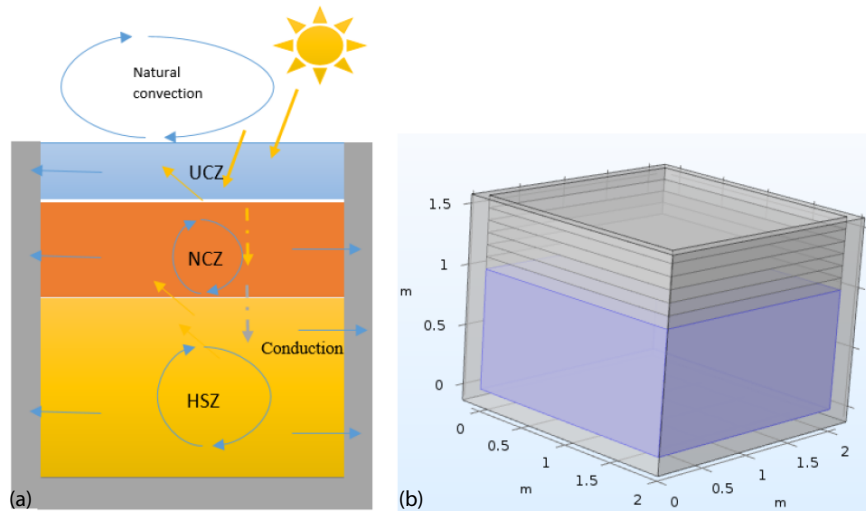


**Figure 1. Schematic design of solar ponds; (a) general lay out of 2-D solar pond, (b) the 3-D model for this study**

In this study, a model solar pond with  $2 \times 2$  m width and depth and 1.6 m height was modelled. Commercial software COMSOL was used to generate the computational mesh. Numerical solution was carefully tested in preliminary calculations and fine mesh with tetrahedral types was applied and mesh density increased to find compatible result with the experimental observations. Mesh distribution is given fig. 2.

Solar position of the sun was arranged and this option is used to estimate external radiative heat source due to the direct striking of the sun rays. Co-ordinates were defined for a Mediterranean city of Adana. Geographical co-ordinates in decimal degrees are (WGS84) latitude of 37.002, longitude of 35.329. Temperature data were taken from General Directorate of Meteorology which has been measured since 1927. Daily average temperature data was defined to system. The ambient temperature follows a simple 24-hour periodic sinusoidal distribution around an average temperature [19] and defined with eq. (1) [20]:

$$T_{\text{amb}} = T_{\text{avg}} + \Delta T \cos\left(2\pi \frac{t-14}{24}\right) \quad (1)$$

where  $T_{\text{avg}}$  and  $\Delta T$  are average temperature and half diurnal temperature variation, respectively,  $t$  – the time in hours, and  $T_{\text{amb}}$  – the ambient temperature. Although the inner zone is prevented from mixing with the upper layers due to the density difference, heat losses in addition to conduction and convection, the third mechanism for heat transfer is radiation. Every object radiates over than the zero-absolute temperature, and this condition manifests itself as heat loss for a

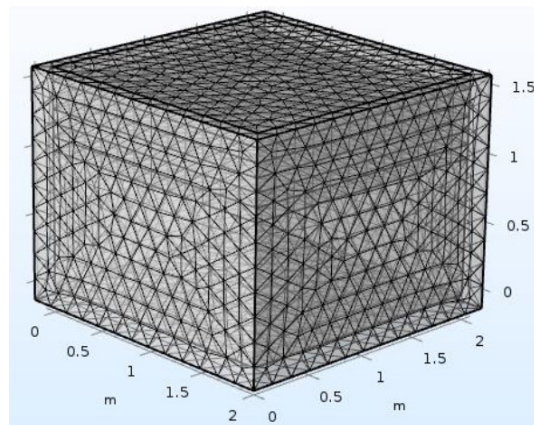


**Figure 2. Mesh distribution for the model solar pond**

solar pond. As the temperature in the zones increases, the heat loss through the radiation is directly proportional to forth power of the temperature and defined with the eq. (2):

$$J = \rho G + \varepsilon n^2 \sigma T^4 \quad (2)$$

where  $\varepsilon$  is emissivity,  $\rho$  – the reflectivity,  $n$  – the refractive index,  $\sigma$  – the absorptivity, and  $T$  – the temperature. Radiosity is the sum of reflected and emitted radiation and denoted  $J$ . The total incoming radiative flux at a point is called irradiation and denoted  $G$ . The surface properties of radiation, emissivity and absorption may depend on the emission or absorption angle, surface temperature or radiation wavelength [21]. For both the rays coming from the sun and the thermal rays radiating from the inside, they interact with the surfaces are not completely transparent and the radiation rays interact with the medium. Different kinds of interaction happen such as absorption, emission and scattering. Let  $I(\Omega)$  represent radiative intensity in a given direction. Some of the radiation is absorbed, some amount of radiation is reflected and part of radiation is scattered depend on interaction coefficient. The balance of the radiative intensity including all contributions (propagation, emission, absorption, and scattering) can now be formulated [20]:

$$\Omega \nabla I(\Omega) = \kappa I_b(T) - \beta I(\Omega) + \frac{\sigma_s}{4\pi} \int_{4\pi} I(\Omega') \varphi(\Omega', \Omega) d\Omega' \quad (3)$$

where  $I(\Omega)$  is the radiative intensity,  $I_b(T)$  – the blackbody radiative intensity,  $\kappa$  – the absorption coefficient,  $\varphi(\Omega', \Omega)$  – the scattering phase function,  $\beta$  – the extinction coefficients. Therefore, both the thermal energy that comes from the Sun and the amount of energy lost from the pond with radiation are calculated with the help of eq. (3). In order to couple the radiation in the participant media, the radiation heat flux is taken into account in addition to the conductive heat flux for the side wall, ground and other brine zone. For the conductive heat transfer in the solid interface can be formulated:

$$\rho C_p \left( \frac{\partial T}{\partial t} + \bar{u}_{\text{trans}} \nabla T \right) + \nabla \cdot (\bar{q} + \bar{q}_r) = -\alpha T : \frac{d\mathbf{S}}{dt} + Q \quad (4)$$

where  $\rho$  is the density,  $C_p$  – the specific heat capacity,  $T$  – the absolute temperature,  $\bar{u}_{\text{trans}}$  – the velocity vector of translational motion,  $\bar{q}$  – the heat flux by conduction,  $\bar{q}_r$  – the heat flux by radiation,  $\alpha$  – the coefficient of thermal expansion,  $\mathbf{S}$  – the second Piola-Kirchhoff stress tensor, and  $Q$  contains additional heat sources. For the conductive heat transfer in the liquid interface can be formulated:

$$\rho C_p \left( \frac{\partial T}{\partial t} + \bar{u} \nabla T \right) + \nabla \cdot (\bar{q} + \bar{q}_r) = -\alpha_p T \left( \frac{dp}{dt} + \bar{u} \nabla p \right) + \boldsymbol{\tau} : \nabla \bar{u} + Q \quad (5)$$

where  $\boldsymbol{\tau}$  is the viscous stress tensor,  $p$  – the pressure,  $\alpha_p$  – the coefficient of thermal expansion. For this study, radiation transfer equation for participating media approximated with discrete ordinates method. When this method is selected opaque surface and continuity in interior boundary are automatically added to the future of model. From the setting page of opaque surface boundary, surface emissivity constant was automatically defined from materials and wall types was set to gray wall. Refractive index was taken 1 and performance index was set to 0.4 for the radiation discretization method. As the performance index value decreases, a robust setting for the solver is expected. Angular discretization of the radiative intensity direction, S4

option was selected. The discrete ordinates method provides a discretization of angular space into  $n = N(N + 2)$  in 3-D discrete directions. In 3-D, S2, S4, S6, and S8 generate 8, 24, 48, and 80 directions [20]. Meteorological data (ASHRAE 2013) was set for ambient variables. The environmental variables like temperature, pressure, humidity *etc.*, were calculated from monthly and hourly average measurements made over several years at weather stations around the world. The ambient data in the heat transfer interfaces was obtained by processing the data measured from the ASHRAE Weather Data Viewer 5.0. The UCZ was modeled as pure water, and the salt concentration of another zone increased by  $30 \text{ kg/m}^3$  in each layer starting from  $1030 \text{ kg/m}^3$ . Relationship between salt density and depth of solar pond and ambient data for soil temperature are given in fig. 3.

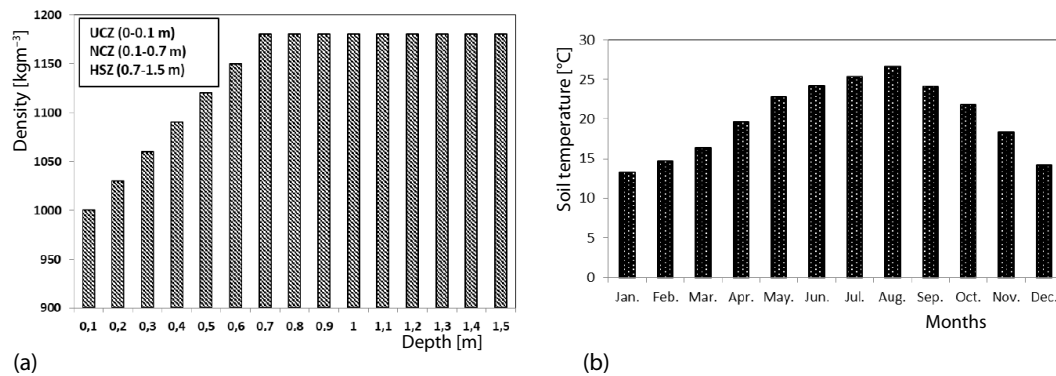


Figure 3. Salt density vs. depth of solar pond (a) and ambient data for soil (b)

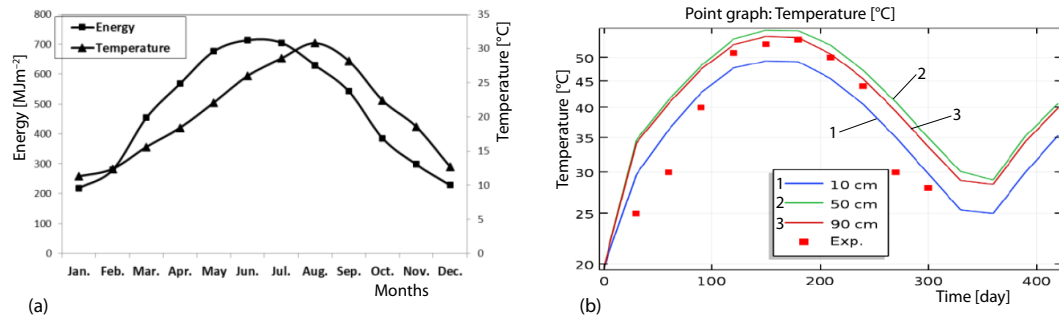
Solar radiation was modeled to absorb 10% of radiation in each layer and the left of it is to be absorbed in HSZ. The solar pond was insulated with glass wool. The thermophysical properties of materials for this model are given in tab. 1.

Table 1. Thermophysical properties of materials used in the model [22]

Material	Water	Salinity water	Stainless steel	Glass-wool
Density [ $\text{kgm}^{-3}$ ]	1000	1100	–	24-96
Heat conductivity [ $\text{Wm}^{-1}\text{°C}^{-1}$ ]	0.6	5.4	17	0.033-0.044
Heat capacity [ $\text{Jkg}^{-1}\text{°C}^{-1}$ ]	4180	850	1000	62

## Results and discussion

In this study, 3-D solar ponds were investigated numerically for different situations, and the consistency of this study was tested by comparing the calculated data with the experimental measurements. Both experimental and numerical studies on solar ponds have been conducted since 2005 district of Adana in Turkey [23, 24]. When examining other localities across Turkey, there has not been extensive studies on solar ponds outside the Adana. Therefore, the meteorological data of Adana were used and is given in fig. 4(a). Seasonal temperature variation was calculated at the height of 10 cm, 50 cm, and 90 cm, respectively from the floor of the solar pond in the HSZ and presented in fig. 4(b). Numerical calculations were conducted starting on the first day of March for 420 days in total, at intervals of 30 days. Figure 4(b) shows that both the experimental and the theoretical results are seasonally changed and the highest value is reached in August at around  $55 \text{ °C}$ . According to data, numerical results range from  $25 \text{ °C}$



**Figure 4. Meteorological data of Adana (a) and Seasonal temperature distribution in the inner zone of solar pond (b)**

to 30 °C, while experimented at 15° and 20° centigrade in January and February, respectively. Therefore, since the data of January and February are well below the numerical data, they are not seen in the graph. However, it is observed that the experimental measurements are in a good agreement with the theoretical data in May to October and the experimental data are slightly below the theoretical calculation results in March to April and November to December.

The temperature distribution in the solar pond was calculated for each month and are given in fig. 5. Numerical calculation was started on the first day of March and continued for one year. The initial temperature of the solar pond was set to 19.6 °C. At the end of the first 30 days the temperature rose by about 15 °C and reached a maximum of 34 °C as seen in fig. 5(a). Maximum temperature then increased by 6° at the end of April to 40 °C, in fig. 5(b), at the end of May, it rose to 48 °C. At the end of June, it increased only by 2 °C and the maximum temperature reached 50 °C and finally at the end of July temperature rose by 5 °C to 55 °C, in figure 5(e), and maintained a maximum of 55 °C in August and no appreciable temperature increase was observed. There was a 5 °C reduction in each month from September to January. At the end of September, it decreased by 5 °C and the maximum temperature become 50 °C, in fig. 5(g), at the end of October it become 45 °C, in fig. 5(h), In November and December temperature continued to decrease and maximum temperatures were calculated 40 °C, in fig. 5(i), and 35 °C, in fig. 5(j), respectively. In January, the temperature decreased by 5 °C and reached 30 °C, in figure 5(k), In February temperature decreased by 2 °C and becomes minimum at 28 °C, in fig. 5(l).

The model solar pond insulated with glass wool was numerically investigated for the subsoil and oversoil conditions and is given in fig. 6. Maximum temperature in the summer season was calculated at around 52 °C in oversoil pond, while it approaches 55 °C in the subsoil case. In the first case, the side walls are in contact with the air. In the latter case, the side walls are in contact with the soil. Temperature difference is caused by different heat transfer coefficients of soil and air. On the other hand, in the winter season, maximum temperature was calculated in the subsoil case higher than the oversoil condition.

Seasonal temperature distribution of solar pond for uninsulated conditions was calculated for subsoil and oversoil case and are given in fig.7. For this part, side walls defined as concrete and wall is in contact with air in the first case and in the second case it is in contact with soil. In oversoil conditions where the temperature change very sharply with respect to seasonal change while in the case of subsoil, variations of temperature appears to be softer. The maximum temperature was calculated at 46 °C in the oversoil and the lowest temperature is 10 °C while in the subsoil case, maximum temperature was calculated at around 33 °C, and minimum at 23 °C. When the maximum temperature values are compared with respect to

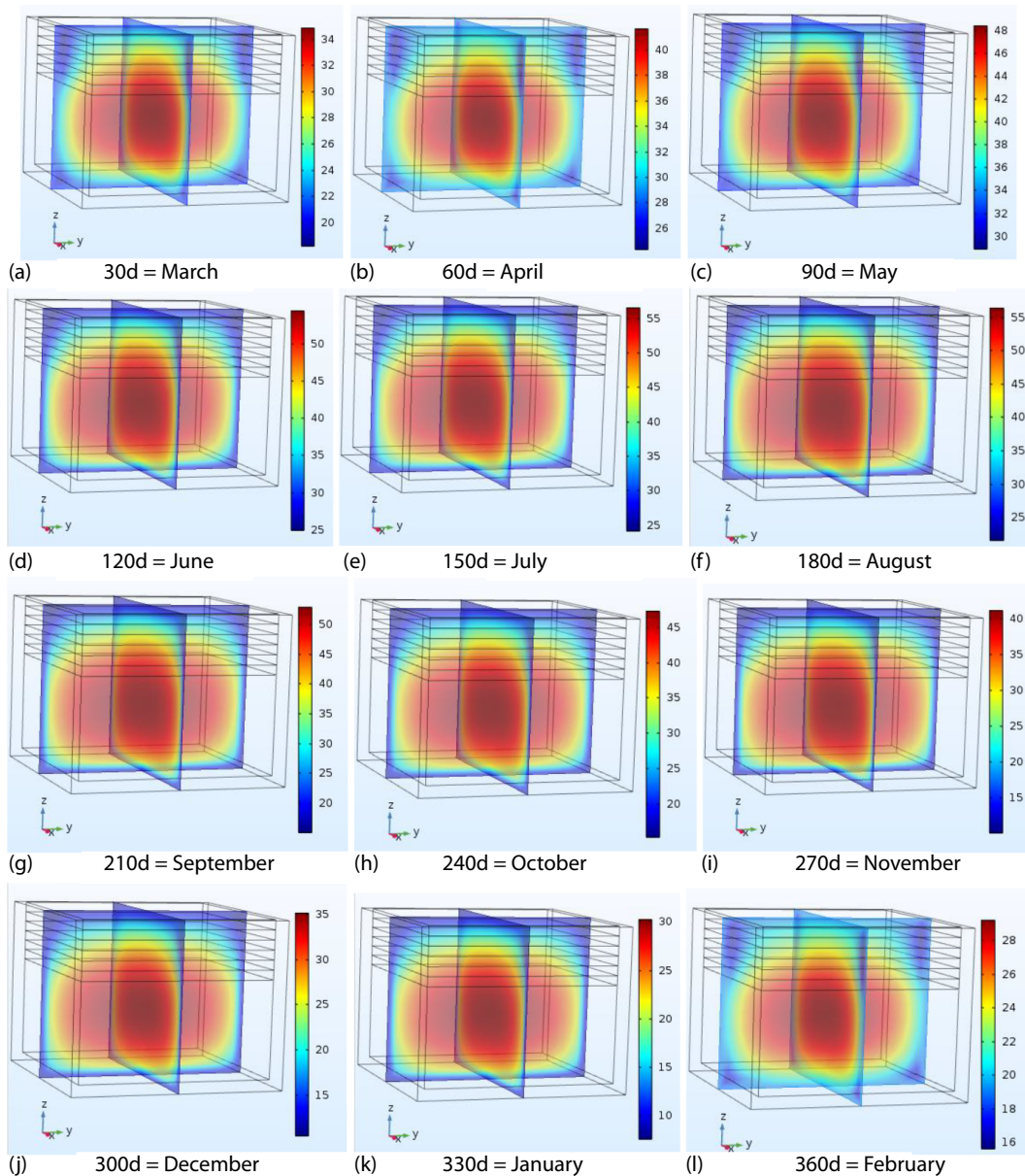


**Figure 5. Seasonal temperature distribution of solar pond by months**  
 (for color image see journal web site)

insulated condition, there is 10 °C difference for the oversoil and 22 °C for the subsoil case. Although the temperature data in the subsoil was simulated lower, but it is seen that the subsoil pond temperature is maintained throughout the year and the change is less.

Seasonal temperature distribution of solar pond for insulated conditions with glass cover was calculated and are given in fig.8. The maximum temperature in the oversoil pond was calculated as 58 °C while in subsoil ponds is 60 °C and maximum temperature was changed by

5 °C compared to open on conditions. Solar pond temperature for oversoil is consistent with the seasonal temperature change but it is maintained under the ground case.

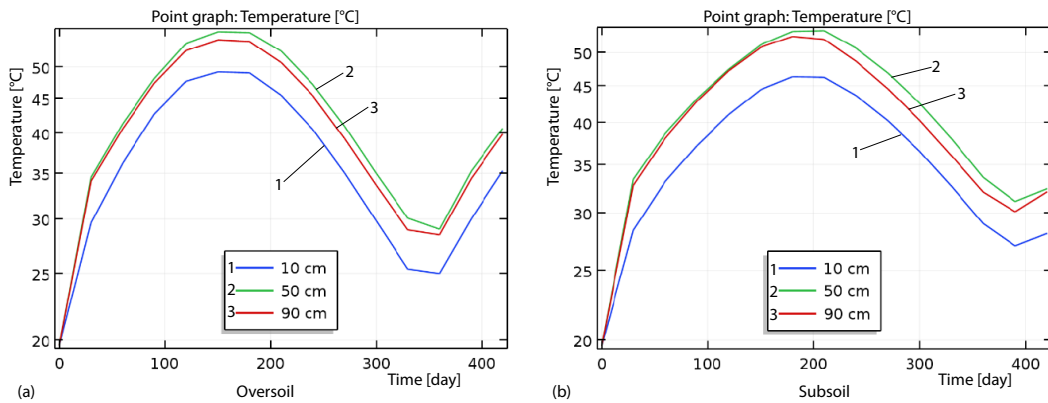


Figure 6. Seasonal temperature distribution of solar pond for insulated conditions

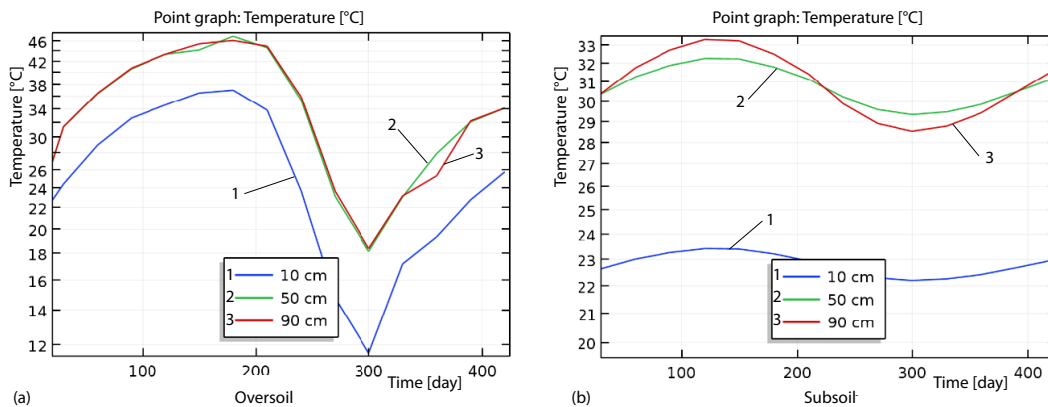


Figure 7. Seasonal temperature distribution of solar pond for uninsulated conditions

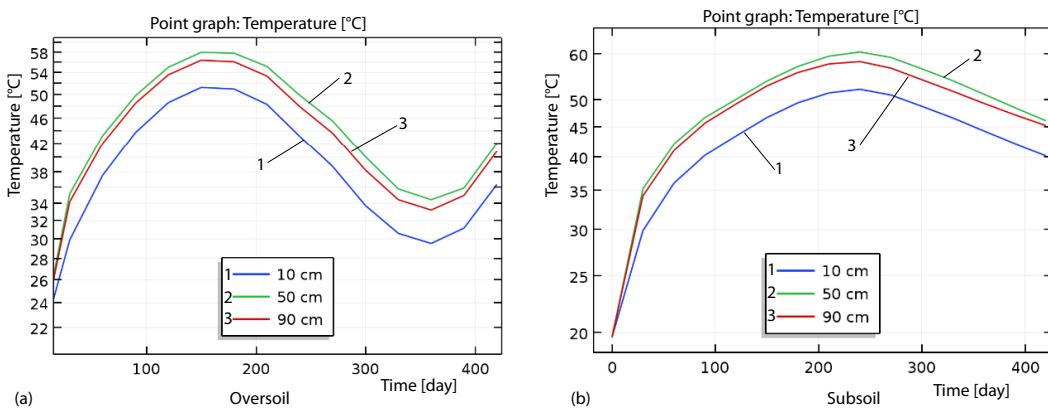


Figure 8. Seasonal temperature distribution of solar pond for insulated conditions with glass cover

## Conclusion

This paper provides numerical investigation of 3-D salt gradient solar pond in Mediterranean climate conditions. Present work demonstrates seasonal temperature distribution of solar pond for the case insulated and uninsulated, with and without cover option for subsoil and oversoil solar pond. First, numerical investigation was conducted for oversoil model solar pond by applying climatic condition for district Adana and obtained data was compared with experimental observation conducted same district to validate simulation accuracy of numerical approaches. There is a good correlation between simulation and experiment especially in summer time. Next, numerical calculation was performed for the insulated and uninsulated, and upper surface of the pond is covered with glass or open to air. Temperature distribution of the insulated pond is rather high compared to the uninsulated case and temperature distribution of the oversoil pond varies according to seasonal variation. Although the maximum temperature point of the subsoil pond is lower than that of the oversoil, it is observed that the temperature change in the subsoil pond is realized less than other, which ensures that heat is retained even more during the winter season. Finally, if the hot water is to be stored for a long periods of time, the subsoil pond is more advantageous in terms of energy efficiency. If hot water is to be used continuously, it is more advantageous in terms of efficiency to build it on the oversoil.

## Acknowledgment

Many thanks to Middle East Technical University and Adiyaman University for technical support.

## Nomenclature

$C_p$	– specific heat capacity at constant pressure, [ $\text{Jkg}^{-1}\text{K}^{-1}$ ]
$I(\Omega)$	– radiative intensity at a given position following the $\Omega$ -direction, [ $\text{W}(\text{m}^2\cdot\text{sr})^{-1}$ ]
$I_b(T)$	– blackbody radiative intensity, [ $\text{W}(\text{m}^2\cdot\text{sr})^{-1}$ ]
$Q$	– heat sources other than viscous heating, [ $\text{Wm}^{-3}$ ]
$\bar{q}$	– heat flux by conduction, [ $\text{Wm}^{-2}$ ]
$q_r$	– heat flux striking the wall, [ $\text{Wm}^{-3}$ ]
$S$	– strain-rate tensor, [ $\text{s}^{-1}$ ]
$s$	– scattering coefficients, [ $\text{m}^{-1}$ ]
$T$	– absolute temperature, [ $\text{K}$ ]
$\bar{u}$	– velocity vector, [ $\text{ms}^{-1}$ ]

## Greek symbols

$\beta$	– extinction coefficients, [ $\text{m}^{-1}$ ]
$\kappa$	– absorption coefficients, [ $\text{m}^{-1}$ ]
$\rho$	– density, [ $\text{kgm}^{-3}$ ]
$\sigma$	– Stefan-Boltzmann constant, [ $\text{JK}^{-1}$ ]
$\tau$	– Cauchy stress tensor deviatoric, [ $\text{Pa}$ ]
$\varphi(\Omega', \Omega)$	– scattering phase function, [–]

## Acronyms

HSZ	– heat storage zone
NCZ	– non-convective zone
UCZ	– upper convective zone

## References

- [1] Simic, M., George, J., Design of a System to Monitor and Control Solar Pond: A Review, *Energy Procedia*, 110 (2017), Mar., pp. 322-327
- [2] Mekhilef, S., et al., A Review on Solar Energy Use in Industries, *Renewable and Sustainable Energy Reviews*, 15 (2011), 4, pp. 1777-1790
- [3] Khalilian, M., Assessment of the Overall Energy and Exergy Efficiencies of the Salinity Gradient Solar Pond with Shading Effect, *Solar Energy*, 158 (2017), Dec., pp. 311-320
- [4] Karakilcik, M., et al., Performance Assessment of a Solar Pond with and without Shading Effect, *Energy Conversion and Management*, 65 (2013), Jan., pp. 98-107
- [5] Bozkurt, I., Karakilcik, M., The Effect of Sunny Area Ratios on the Thermal Performance of Solar Ponds, *Energy Conversion and Management*, 91 (2015), Feb., pp. 323-332
- [6] Moh'd, A. A. N., Al-Dafaie, A. M. A., Using Nanofluids in Enhancing the Performance of a Novel Two-Layer Solar Pond, *Energy*, 68 (2014), Apr., pp.318-326

- [7] Munoz, F., Almanza, R., A Survey of Solar Pond Developments, *Energy*, 17 (1992), 10, pp. 927-938
- [8] Sakhrieh, A., Al-Salaymeh, A., Experimental and Numerical Investigations of Salt Gradient Solar Pond under Jordanian Climate Conditions, *Energy Convers Manag*, 65 (2013), Jan., pp. 725-728
- [9] Karakilcik, M., *et al.*, Experimental and Theoretical Temperature Distributions in a Solar Pond, *Int. J. Heat Mass Transf.*, 49 (2006), 5-6, pp. 825-835
- [10] Bozkurt, I., *et al.*, A New Performance Model to Determine Energy Storage Efficiencies of a Solar Pond, *Heat Mass Transfer*, 51 (2015), 1, pp. 39-48
- [11] Sogukpinar, H., *et al.*, Numerical Evaluation of the Performance Increase for a Solar Pond with Glazed and Unglazed, *Proceedings*, IEEE International Conference on Power and Renewable Energy, Shanghai, China, 2016, pp. 598-601
- [12] Sogukpinar, H., *et al.*, Performance Comparison of Aboveground and Underground Solar Ponds, *Thermal Science*, 22 (2018), 2, pp. 953-961
- [13] Bozkurt, I., *et al.*, Modeling of a Solar Pond for Different Insulation Materials to Calculate Temperature Distribution, *Journal of Multidisciplinary Engineering Science and Technology*, 2 (2015), 6, pp. 1378-1382
- [14] Chekerovska, M. Filkoski, R.V., Efficiency of Liquid Flat-Plate Solar Energy Collector with Solar Tracking System, *Thermal Science*, 19 (2015), 5, pp. 1673-1684
- [15] Ding, L. C., *et al.*, Transient Model to Predict the Performance of Thermoelectric Generators Coupled with Solar Pond, *Energy*, 103 (2016), May, pp. 271-289
- [16] Ali, H. M., Mathematical Modelling of Salt Gradient Solar Pond Performance, *Int. J. Energy Res.* 10 (1986), 4, pp. 377-384
- [17] Sayer, A. H., *et al.*, New Theoretical Modelling of Heat Transfer in Solar Ponds, *Sol. Energy*, 125 (2016), Feb., pp. 207-218
- [18] Chiasson, A. D., *et al.*, A Model for Simulating the Performance of a Shallow Pond as Supplemental Heat Rejecter with Closed-Loop Ground-Source Heat Pump Systems, *ASHRAE Trans.*, 106 (2000), Jan., pp. 107-121
- [19] \*\*\*, Heat Transfer Module, COMSOL. <https://www.comsol.com> [accessed 10 May 2018]
- [20] Modest, M. F., *Radiative Heat Transfer*, 2<sup>nd</sup> ed., Academic Press, San Diego, Cal., USA, 2003
- [21] Sieger, R., Howell, J., *Thermal Radiation Heat Transfer*, Taylor & Francis, 4<sup>th</sup> ed., New York, USA, 2002
- [22] Mantar, S., A Mathematical Modeling of the Insulated Cylindrical Model Solar Ponds (in Turkish), MSc. thesis, Cukurova University, Adana, Turkey, 2010
- [23] Karakilcik, M., *et al.*, Performance Investigation of a Solar Pond, *Applied Thermal Engineering*, 26 (2006), 7, pp. 727-735
- [24] Bozkurt, I., Karakilcik, M., The Daily Performance of a Solar Pond Integrated with Solar Collectors, *Solar Energy*, 86 (2012), 5, pp.1611-1620